Magnetohydrodynamics Stability of Compact Stellarators

G. Y. Fu[a], L. P. Ku[a], W. A. Cooper[b], S. H. Hirshman[c], D. A. Monticello[a], M. H. Redi[a], A. Reiman[a], R. Sanchez[d], D. A. Spong[c]

[a] *Princeton Plasma Physics Laboratory, Princeton, New Jersey 08543*

[b] *CRPP, EPFL, Lausanne, Switzerland*

[c] *Oak Ridge National Laboratory, Oak Ridge, Tennessee 37830*

[d] *Universidad Carlos III de Madrid, Madrid, Spain*

(December 20, 1999)

Abstract

Recent stability results of external kink modes and vertical modes in compact stellarators are presented. The vertical mode is found to be stabilized by externally generated poloidal flux. A simple stability criterion is derived in the limit of large aspect ratio and constant current density. For a wall at infinite distance from the plasma, the amount of external flux needed for stabilization is given by $F_i = (\kappa^2 - \kappa)/(\kappa^2 + 1)$, where κ is the axisymmetric elongation and F_i is the fraction of the external rotational transform. A systematic parameter study shows that the external kink mode in QAS can be stabilized at high beta ($\sim 5\%$) without a conducting wall by magnetic shear via 3D shaping. It is found that external kinks are driven by both parallel current and pressure gradient. The pressure contributes significantly to the overall drive through the curvature term and the Pfirsch-Schluter current.

I. INTRODUCTION

The design of the proposed National Compact Stellarator Experiment(NCSX) [1–3] aims at combining the best features of both tokamak and stellarator to achieve reactor-relevant plasma performance: high beta, good particle confinement, disruption-free steady state operation with little need for current drive, and compact size. The NCSX is based on the concept of a quasi-axisymmetric stellarator (QAS) [4,5]. Quasi-axisymmetry denotes a magnetic field strength that is approximately axisymmetric in Boozer coordinate, hence the particle confinement of a quasi-axisymmetric device is nearly as good as that of an axisymmetric tokamak. Our QAS configurations are obtained from tokamaks by adding rotational transform generated by 3D shaping (nonaxisymmetric coils) in such a way that the Boozer spectrum of field strength is approximately axisymmetric.

At high beta, quasi-axisymmetry necessarily leads to substantial bootstrap currents. The bootstrap current generates an internal rotational transform which always adds to the externally generated transform. This large current helps to generate poloidal flux needed for good confinement, but it may also destabilize kink modes as in tokamaks. In this work, we investigate the stability of ideal Magnetohydrodynamics(MHD) modes, such as external kink modes and vertical mode, in QAS.

Early work considered current-driven external kink modes and recognized the stabilizing role of magnetic shear [6–8]. More recently, Mikhajlov and Shafranov [9] have shown analytically that a sufficient magnetic shear generated by helical coils can stabilize the external kink modes. With only a few exceptions [10,11], previous work on current-driven kinks assumed large aspect ratio and low beta. More recently, Johnson *et al.* [11], assuming large aspect ratio, found that the effects of bootstrap current on kinks are strongly destabilizing at finite beta in the Large Helical Device (LHD) [12]. In other work, Ardelea and Cooper [10] found that external kink modes in tokamaks can be stabilized by 3D deformation for $q < 2$ at moderate beta values ($\beta < 2\%$). In this work, we use fully 3D calculations for high beta compact stellarators where the external kinks are driven by both bootstrap current and

pressure gradient.

We find that external kink modes in high beta QAS can be stabilized by global and local magnetic shear using appropriate 3D shaping without a conducting wall. In contrast, advanced tokamaks with high bootstrap fraction tend to have much lower beta limits without wall stabilization. Initial results of external kink stability in QAS have been reported elsewhere [13]. Here the stability results are refined by using more Fourier harmonics for the perturbation.

Here, we also study for the first time the vertical mode in QAS configurations. We find that highly shaped QAS configurations are much more stable to vertical modes than tokamaks. Physically, this is because the externally generated poloidal flux enhances the field line bending energy relative to the current-driven term.

In addition to QAS, we have recently investigated the MHD stability in Quasi-Omnigeneous Stellarators (QOS) [3,14]. QOS devices are ones where the contours of the second adiabatic invariant $J = \int v_{\|} dl$ approximately coincide with magnetic flux surfaces so that the trapped particle orbit deviation from flux surfaces is minimal and the particle confinement is much improved over that of conventional stellarators. QOS configurations typically have much larger helical component than QAS configurations. One consequence of this is that in QOS devices the bootstrap current is smaller than that of QAS devices because of cancellation between the $n = 0$ component and $n \neq 0$ components of the bootstrap current. Also, the bootstrap current can be of either sign so it can add to, or subtract from, the vacuum rotational transform. For the compact QOS configuration considered here, the bootstrap current subtracts from the vacuum transform. This negative bootstrap current is shown to lead to kink stability for monotonic increasing iota profile.

II. THE 3D STABILITY CODE TERPSICHORE

In this work, the three dimensional ideal MHD stability code Terpsichore [15] is used to calculate the stability of free boundary external kink modes. The code determines the

eigenvalues of the ideal MHD equations by minimizing the plasma potential energy as defined in the energy principle [16],

$$\omega^2 \delta W_k = \delta W_p + \delta W_{vac} \tag{1}$$

where δW_p is the plasma potential energy, δW_{vac} is the magnetic energy in the vacuum region between plasma and conducting wall, and $\omega^2 \delta W_k$ is the kinetic energy. An explicit form of δW_p will be given in Sec. III. The Terpsichore code takes as input full 3D numerical equilibria obtained by the VMEC [17] code. It uses a finite hybrid element method for radial discretization and Fourier decomposition in poloidal and toroidal angles. The radial and surface component of the plasma displacement vector ξ is represented by

$$\xi^s(s,\theta,\phi) = \sum_l \xi_l(s) \sin(m_l\theta - n_l\phi + \delta) \tag{2}$$

$$\eta(s,\theta,\phi) = \sum_l \eta_l(s) \cos(m_l\theta - n_l\phi + \delta) \tag{3}$$

where $\xi^s = \xi \cdot \nabla s$ and $\eta = \xi \cdot \mathbf{B} \times \nabla s / |\nabla s|^2$ with s being the flux variable. It should be pointed out, that in the present study, an artificial kinetic energy is used for simplicity. This artificial kinetic energy is given by $\delta W_k = (1/2) \int d^3x [(\xi^s)^2 + (\eta)^2]$. As a result, the calculated eigenvalue does not correspond to the physical growth rate. However, the marginal stability boundary remains the same.

Assuming stellarator symmetry with field period N_p, modes with mode number n are coupled to $n + kN_p$, where k is an arbitrary integer. There are $N_p/2 + 1$ families for even N_p and $(N_p - 1)/2 + 1$ families for odd N_p. For example, there are $n = 0$ and $n = 1$ families for $N_p = 3$ and there are $n = 0$, $n = 1$ and $n = 2$ families for $N_p = 4$. Usually, the $n \neq 0$ families are called kink modes and $n = 0$ family is called vertical mode. However, when the dominating component is of $n \neq 0$, the $n = 0$ family of modes are more characteristic of kink modes than vertical modes and we will refer to them as such.

It can be shown that the stability of $n \neq 0$ families does not depend on the phase δ except for the $n = N_p/2$ family when N_p is even. The phase is zero for the vertical mode of the $n = 0$ family.

The Terpsichore code has been benchmarked extensively. Earlier it was shown [18] that the Terpsichore's stability results agree well with other stability codes for growth rates of fixed boundary MHD modes in 2D analytic Solov'ev equilibria. In the present work, we have benchmarked Terpsichore against the 2D stability code PEST [19] and the 3D code CAS3D [20] for external kink modes for an optimized reversed shear tokamak equilibrium from the ARIES studies [21]. The calculated beta limit of the $n = 1$ external kink mode using Terpsichore is 2.34%, which agrees well with the PEST result of 2.4% and the CAS3D result of 2.3% [22]. We have also benchmarked the code for the $n = 0$ vertical mode in a large aspect ratio tokamak plasma. Figure 1 plots the critical wall radius as function of ellipticity for the stability of the $n = 0$ vertical mode in an elliptical plasma with constant current density profile and zero beta. The Terpsichore results (shown in dots) agree well with the analytic stability criterion [23] (solid line) give by

$$r_w = \sqrt{\frac{\kappa + 1}{\kappa - 1}} \tag{4}$$

where the normalized wall radius is defined by $r_w = (a' + b')/(a + b)$ with a and b (a' and b') being the radius of the elliptical plasma (a confoncal wall) along the horizontal and vertical direction respectively. Here, $\kappa = b/a$.

III. STABILITY OF EXTERNAL KINK MODE

We consider the stability of low-n external kink modes driven by current and pressure using the Terpsichore code. A systematic convergence study has been done in terms of the number of equilibrium harmonics, number of radial grid points, and number of Fourier harmonics for perturbations. Results show that kink eigenvalues converge quadratically in radial grid size and exponentially in number of equilibrium and stability harmonics. In particular, Fig. 2 shows the exponential convergence of the eigenvalue of a n=1 external kink mode in number of stability harmonics. The results are obtained for a $N_p = 3$ QAS with $R/a = 3.5$ and $\beta \sim 4\%$. These results indicate that a resolution of about 50 grid

points, 100 equilibrium harmonics and 100 stability harmonics is required for typical QAS under considerations.

We now consider the effects of magnetic shear on external kink stability. Figure 3 shows the calculated n=1 external kink mode eigenvalue $\lambda = -\omega^2$ as a function of global magnetic shear near the edge defined by $\iota(1) - \iota(0.75)$ at $\iota(1) = 0.46$. It is seen that the external kink mode is stabilized by edge magnetic shear. These results are obtained for a $N_p = 4$ QAS with $R/a = 2.1$ and $\beta \sim 6.3\%$. The variation of shear is controlled entirely by 3D plasma boundary shape. The current and pressure profiles are fixed.

However, a complete stabilization by global shear alone tends to reduce central rotational transform to low values (~ 0.1) and result in poor particle confinement. This problem can be solved by further 3D shaping that does not affect the global shear. We find that external kinks can be stabilized by appropriate 3D shaping at moderate global shear. In order to find the optimal shaping for kink stability, we have incorporated the Terpsichore code into a configuration optimizer which includes kink stability as well as quasisymmetry in its objective function. The optimizer is used to determine the necessary 3D shaping for kink stabilization. Figure 4 shows plasma cross-sections of a three field period $R/a = 3.5$ QAS before (left) and after (right) the stability optimization. The corresponding rotational transform profiles are shown in Fig. 5. The initial configuration (called c3m) is unstable to an n=1 kink with eigenvalue of $\lambda = 1.8 \times 10^{-3}$. Figure 6 plots the perturbed pressure contour of the corresponding eigenmode at the two symmetric cross-section (at $\phi = 0$ and $\phi = \pi/3$). The unstable mode peaks on the outboard side of the plasma (i.e., ballooning) due to destabilizing bad curvature. The final configuration after optimization (called c82) is marginally unstable with eigenvalue of $\lambda = 2.6 \times 10^{-5}$ at $\beta = 3.9\%$. We note that the change in the iota profile from c3m's to c82's is minimal and the two order of magnitude reduction in kink eigenvalue can only be attributed to the change in 3D shaping. The major change in shaping from c3m to c82 is an indentation of plasma boundary on the outboard side at the half-period cross section which is found to be most effective for stabilization. The optimized configuration c82 is also stable to high-n ballooning modes. It has good quasi-axisymmetry.

The plasma current comes mainly from the bootstrap and contributes about half of the total rotational transform, as shown in Fig. 7. This configuration will be shown to be robustly stable to the vertical mode. Currently, it is one of candidate configurations for NCSX.

The physical mechanisms for the stability of the external kink mode are investigated by examining individual contributions to the plasma potential energy and the effects of 3D shaping on local magnetic shear and normal curvature. To separate out various stabilizing and destabilizing terms in the plasma potential energy, we use the following form of the potential energy:

$$\delta W_p = \frac{1}{2}\int d^3x [\delta \mathbf{B}_\perp{}^2 + (\delta \mathbf{B}_\parallel - \mathbf{B}\frac{\xi\cdot\nabla p}{B^2})^2 + \mathbf{j}_\parallel \cdot \xi \times \delta\mathbf{B} - 2\xi\cdot\nabla p\, \xi\cdot\kappa] \quad (5)$$

where $\delta\mathbf{B}$ is the perturbed magnetic field, $j_\parallel$ is the parallel equilibrium current along the field line, ξ is the plasma displacement vector, and κ is the magnetic curvature. The integration is carried out for the whole plasma region. The first term in the integrand is the stabilizing field line bending energy, the second is the field compression energy, the third term is destabilizing due to parallel current and is responsible for kink instabilities. Lastly, the fourth term is destabilizing due to unfavorable curvature and pressure gradient. Table I list the relative contributions of these terms normalized by the vacuum magnetic energy for both c3m and c82. We note that the parallel current term contributes about 70% of the total destabilizing sum for both cases and is thus the main destabilizing mechanism for the $n = 1$ external kink modes, in accordance with usual expectation. However, the ballooning term also contributes significantly to the instability. This is the reason the mode exhibits the strong ballooning feature as shown in Fig. 6. For c3m, the configuration would be stable if the ballooning term is neglected since the sum of the destabilizing term is only about 13% higher than the sum of stabilizing terms. Thus, the unstable mode should be called kink-ballooning mode. The pressure also contributes indirectly to the kink term through the parallel Pfirsch-Schluter current. For both cases, the Pfirsch-Schluter current contributes about 57% of the kink term. Thus, the pressure-induced Pfirsch-Schlute current is actually more important than

the volume-averaged parallel current for these two configurations.

We now discuss why the 3D shaping change from c3m to c82 stabilizes the external kink mode. We observe from Table I that the main difference between c3m and c82 is the field line bending term. This suggests that the effects of shaping on *local* magnetic shear plays a significant role. Figure 8 shows the contours of local magnetic shear of c82 on the $s = 0.63$ flux surface (the δW_p peaks approximately at this surface). Here, the local magnetic shear $\hat{S}$ is defined by $\hat{S} = -(\sqrt{g}/\Psi'^2)\mathbf{h} \cdot \nabla \times \mathbf{h}$ with $\sqrt{g}$ being the Jacobian and $\mathbf{h} = \mathbf{B} \times \nabla s/|\nabla s|^2$. Note that the global magnetic shear dq/ds is a surface average of $\hat{S}$ where $q = 1/\iota$. The value of local shear in Fig. 8 range from -74.3 to 28.6. while the global shear is $dq/ds = -2.4$. This shows that the local magnetic shear is dominated by helical contribution and is much larger than the global shear. Figure 9 compares the local magnetic shear of c3m with that of c82 on the outboard side at $s = 0.63$. Indeed we find that the local shear of c82 is substantially larger than that of c3m on the outboard side. This indicates that the local shear is responsible for the change in the field line bending energy and the stability between these two configurations.

Recently we have investigated the kink stability in QOS. Initial results show that the external kink modes are stable for a $R/a = 3.6$, $\beta = 3.7\%$ QOS with self-consistent bootstrap current. The bootstrap current is negative and decreases the rotational transform at edge by about 15%. When beta is increased to 5%, the plasma is marginally unstable to an interchange-like mode with weak ballooning feature as shown in the upper plot of Fig. 10. The bootstrap current contribution to this mode is very small (about 10% of the pressure contribution) and the mode is mainly internal. We have examined the effects of bootstrap current direction on kink stability by artificially changing the sign of the current in the δW_p while keeping all other equilibrium quantaities fixed. When the sign of the current is changed to positive, the QOS configuration becomes unstable to a mode with clear external kink features as shown in the lower plot of Fig. 10 (i.e., the mode is external with significant drive from the kink term). This result shows the importance of the sign of bootstrap current, even for relatively small current magnitude. This indicates that the kink stability can be

controlled in a QOS plasma by varying the bootstrap current. In addition to external kink modes, we have also studied the high-n ballooning modes. Our results show that the ballooning modes can be stabilized by 3D shaping and thus the beta limit can be increased from 2% to 4% in one specific case.

Finally, it worth noting the recent work by Johnson *et al.* [11] where the external kink modes were shown to be unstable in LHD at moderate value of beta of $\beta > 2\%$ at zero net current. Addition of the self-consistent bootstrap current was found to strongly enhence the kink growth rate and reduce the beta limit further. As pointed out by the authors, this low beta limit is probably due to the large rotational transform in LHD where $\iota > 1$ for most of the plasma. In contrast, the QAS configurations considered here have much lower transform at $\iota < 0.5$. Simple theory shows that external kink modes are more unstable for smaller resonant poloidal mode numbers associated with higher ι. This explains why external kink modes can be unstable in LHD even at large global magnetic shear.

IV. STABILITY OF VERTICAL MODES

It is known that tokamaks with high elongation suffer from lack of vertical stability which could result in disruptions unless feedback stabilization were employed.

We find that the vertical mode (of $n = 0$ family) can be much more stable in QAS devices than in tokamaks. The configuration c82 is calculated to be robustly stable to the vertical mode. The stability has been confirmed by CAS3D calculations with a conducting wall at infinite [22]. In order to understand the physics, we have evaluated stability for a series of equilibria by varying the degree of nonaxisymmetric shape of c82. Figure 11 shows the eigenvalue of the vertical mode as function of the fraction of nonaxisymmetric shape, f, at fixed current profile and zero beta. Here $f = 1$ corresponds to the full c82 shape and $f = 0$ corresponds a tokamak with the axisymmetric shape of c82. Equilibria are obtained by linear interpolation of the tokamak shape and the c82 shape (i.e., $R_{m,n}(f) = fR_{m,n}$, $Z_{m,n}(f) = fZ_{m,n}$ for $n \neq 0$, where $R_{m,n}$ and $Z_{m,n}$ are Fourier coefficients of the c82 shape).

We observe that there is a large stability margin for the vertical mode in c82 with the marginal point at $f = 0.6$. The results of Fig. 11 are obtained with zero beta because of equilibrium convergence problem due to low ι at small f. At finite f, the effects of beta are found to be stabilizing. Thus, an even larger margin is expected at finite beta.

We have derived an analytic stability criterion for vertical mode in a large aspect ratio QAS with constant current density and constant external rotational transform [24]. The external rotational transform needed for stability is given by:

$$F_i = \frac{\kappa^2 - \kappa}{\kappa^2 + 1} \tag{6}$$

where $F_i = \iota_{ext}/\iota_{total}$ is the fraction of external rotational transform and κ is the axisymmetric elongation. This criterion has been confirmed by the Terpsichore code, as shown in Fig. 12. The calculated critical external transform (solid dots) agrees reasonably well with the analytic result (solid line). Physically, the external transform is stabilizing because the external poloidal flux enhances the field line bending energy relative to the current-driven term for the vertical instability.

V. CONCLUSIONS

The MHD stability properties of current-carrying quasi-axisymmetric stellarators are investigated using full 3D calculations. The vertical mode in quasi-axisymmetric stellarators has been studied for the first time. It is found that the vertical mode is much more stable in QAS than in tokamaks due to stabilizing effects of externally generated poloidal flux. The external kink modes in QAS can be stabilized by global and local magnetic shear via 3D shaping at high beta without a conducting wall. The results found here demonstrate that there exists a new class of stellarators with quasi-axisymmetry, large bootstrap current, compact size that have a high MHD beta limit without a conducting wall.

The authors acknowledge the support of the NCSX team. We acknowledge valuable discussions with Drs. Allen Boozer, Chris Hegna, Steve Jardin, John Johnson, Charles

Kessel, Janardhan Manickam, Wonchull Park, Neil Pomphrey, Mike Zarnstorff. We thank Drs. Rob Goldston and Hutch Neilson for their encouragement and support for this work. This work is supported by the U.S. Department of Energy under Contract No. DE-AC02-76-CHO-3073.

REFERENCES

[1] G. H. Neilson, A. Reiman, M. Zarnstorff *et al.*, "Physics Basis for High-Beta, Low-Aspect-Ratio Stellarator Experiments", submitted to Phys. Plasmas, 1999.

[2] A. Reiman, G. Fu, S. Hirshman *et al.*, "Physics Design of a High β Quasi-Axisymmetric Stellarator", submitted to Plas. Physics and Contr. Fusion, 1999.

[3] S. P. Hirshman, D. A. Spong, J. C. Whitson *et al.*, Phys. Plasmas 6, 1858 (1999)

[4] J. Nuhrenberg, W. Lotz, and S. Gori, *Theory of Fusion Plasmas* (Editrice Compositori Bologna, Bologna, 1994).

[5] P. R. Garabedian, Phys. Plasmas **3**, 2483 (1996).

[6] J. L. Johnson, C. R. Oberman, R. M. Kulsrud, and E. A. Frieman, Phys. Fluids **1**, 281 (1958).

[7] R. M. Sinclair, S. Yoshikawa, W. L. Harries, and K. M. Young, Phys. Fluids **8**, 118 (1965).

[8] K. Matsuoka, K. Miyamoto, K. Ohasa, M. Wakatani, Nuclear Fusion **17**, 1123 (1977).

[9] M. I. Mikhajlov and V. D. Shafranov, Nucl. Fusion **30**, 413 (1990).

[10] A. Ardelea and W. A. Cooper, Phys. Plasmas **4**, 3482 (1997).

[11] J. L. Johnson, K. Ichiguchi, Y. Nakamura, M. Okamoto, M. Wakatani, and N. Nakajima, Phys. Plasmas **6**, 2513 (1999).

[12] A. Ilyoshi, M. Fujiwara, O. Motojima, N. Ohyabu, and K. Yamazaki, Fusion Technology **17**, 169 (1990).

[13] G. Y. Fu, L. P. Ku, N. Pomphrey *et al.*, in the 17th IAEA Fusion Energy Conference, Yokohama, Japan, 19-24 October 1998 (International Atomic Energy Agency, Vienna) Paper IAEA-FI-CN-69/THP1/07.

[14] S. P. Hirshman, D. A. Spong, J. C. Whitson, V. E. Lynch, D. B. Batchelor, B. A. Carreras, and J. A. Rome, Phys. Rev. Lett. **80**, 528 (1998).

[15] D. V. Anderson, W. A. Cooper, R. Gruber, S. Merazzi, and 115 U. Schwenn, Scient. Comp. Supercomputer II, 159 (1990).

[16] I. B. Bernstein, E. A. Frieman, M. D. Kruskal and R. M. Kulsrud, Phys. Fluids, Proc. R. Soc. London Ser. A **244**, 17 (1958).

[17] S. P. Hirshman and J. C. Whitson, Phys. Fluids **26** 3553 (1983).

[18] G. Y. Fu, W. A. Cooper, R. Gruber, U. Schwenn, D. V. Anderson, Phys. Fluids B**4**, 1401 (1992).

[19] R. C. Grimm, J. M. Greene, J. L. Johnson, Methods Comput. Phys. **16**, 273 (1975).

[20] C. Nuehrenberg, Phys. Plas. **3**, 2401 (1996).

[21] S. C. Jardin, C. E. Kessel, C. G. Bathke et. al., Fusion Engr. and Design **38**, 27 (1997).

[22] M. H. Redi, C. Nuehrenberg, W. A. Cooper, G. Y. Fu, C. Kessel, L. P. Ku, the 26th EPS Conference on Controlled Fusion and Plasma Physics, Maastricht, Netherlands, 1999 (The European Physical Society) Paper P4.085.

[23] D. Dobrott and C. S. Chang, Nuclear Fusion **21**, 1573 (1981).

[24] G. Y. Fu, "Vertical Stability in a Current-carrying Stellarator", submitted to Phys. Plasmas.

TABLES

TABLE I. The breakdown of stabilizing and destabilizing terms in the plasma potential energy normalized by the vacuum energy for the most unstable $n = 1$ external kink mode in c3m and c82.

	vacuum	line bending	kink	ballooning
c3m	1.00	4.05	−3.98	−1.72
c82	1.00	4.51	−3.87	−1.64

FIGURES

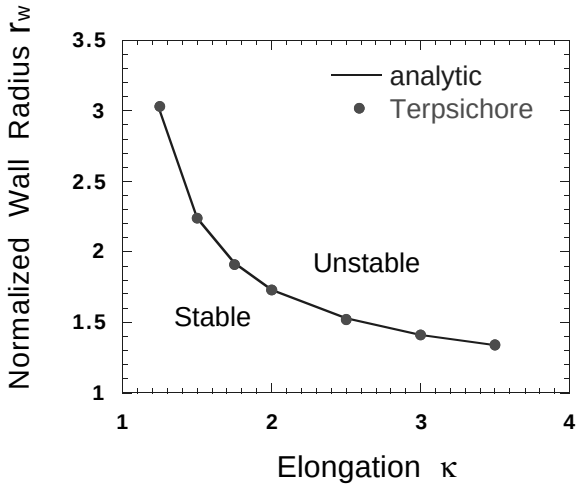

FIG. 1. *The critical normalized wall radius versus elongation for a elliptical plasma.*

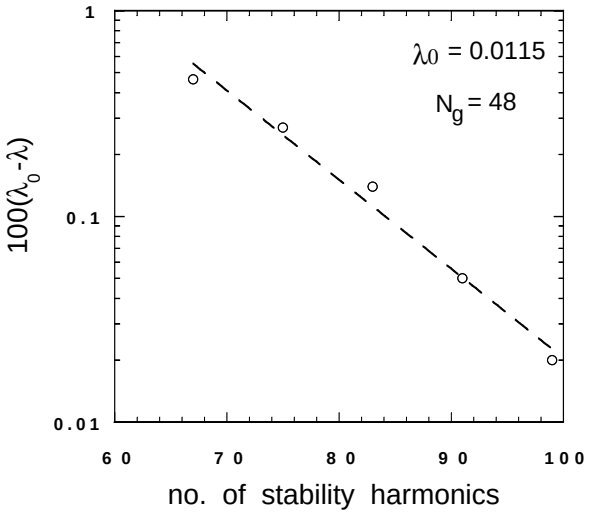

FIG. 2. *The $n = 1$ external kink eigenvalue versus number of stability Fourier harmonics.*

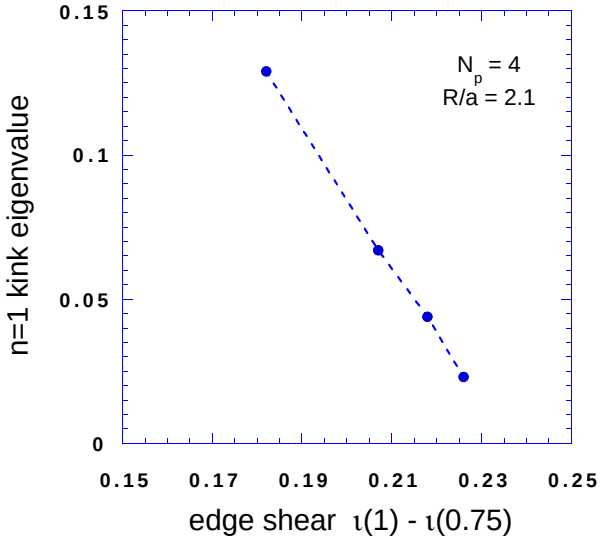

FIG. 3. *The $n = 1$ external kink eigenvalue versus edge magnetic shear for a four field period QAS with $R/a = 2.1$ and $\beta \sim 6.3\%$.*

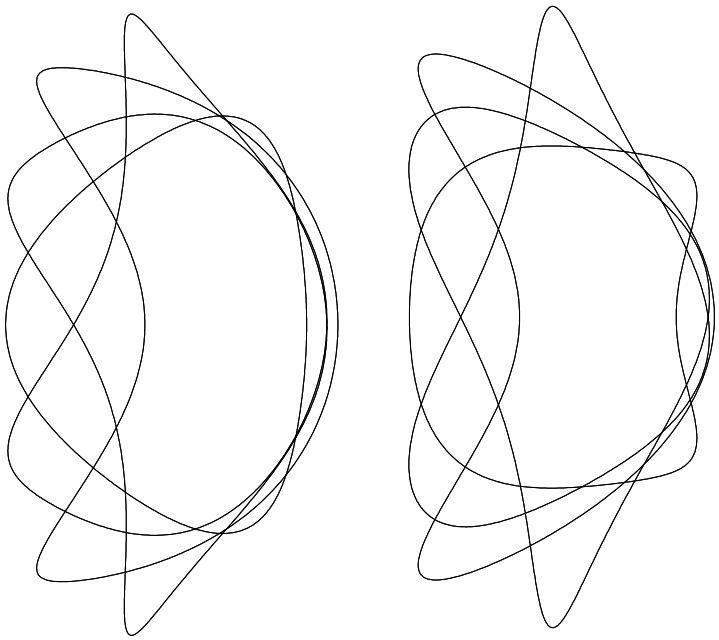

FIG. 4. *Plasma cross-sections of a three field period QAS before optimization (left) and after optimization (right).*

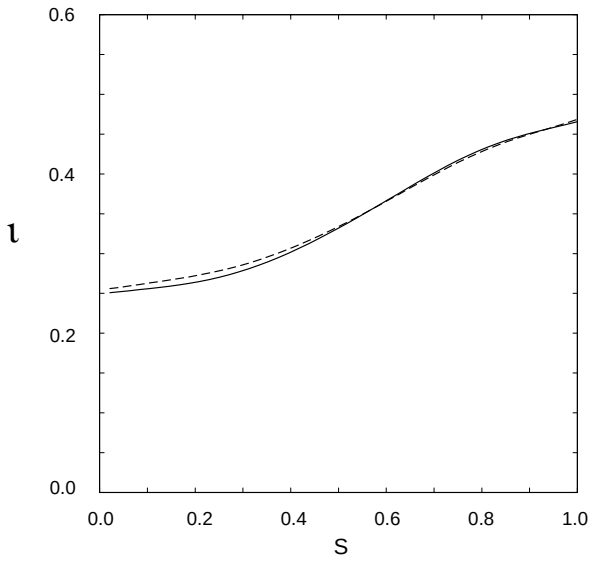

FIG. 5. *Iota profiles of a three field period QAS before optimization (solid line) and after optimization (dashed line).*

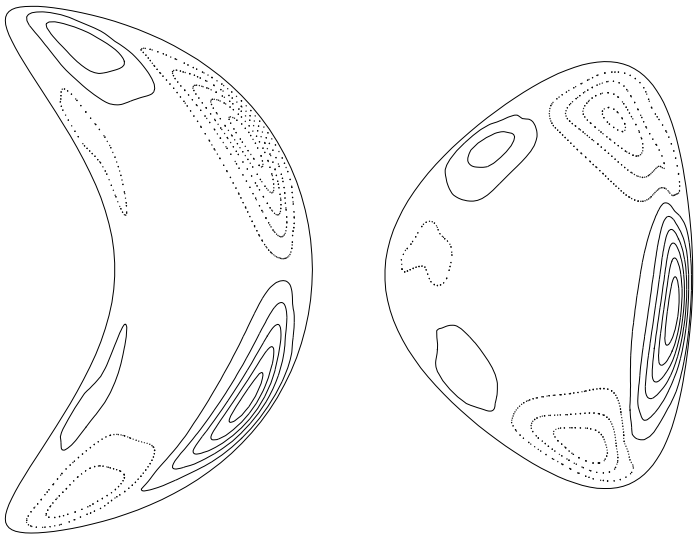

FIG. 6. *contours of perturbed pressure at the two symmetric cross-sections for c3m.*

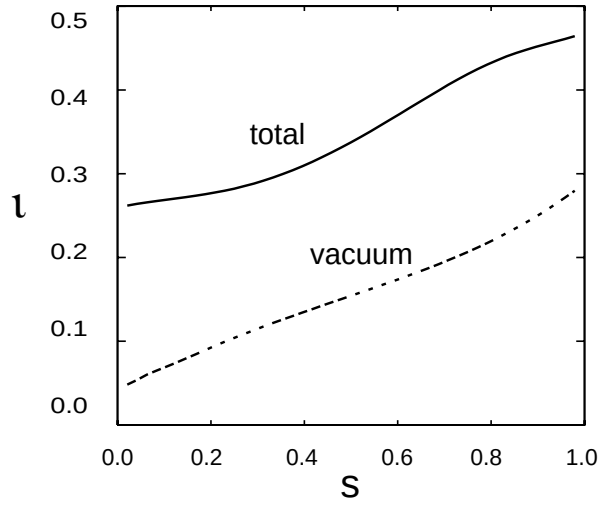

FIG. 7. *The total (solid) and vacuum (dashed) rotational transforms v.s. the normalized toroidal flux s for the configuration c82.*

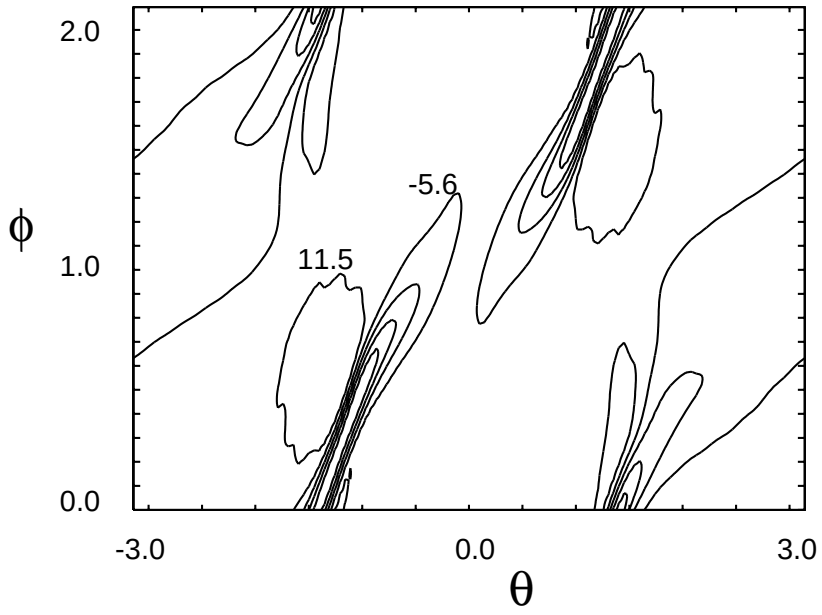

FIG. 8. *The contour plot of the local magnetic shear of the configuration c82 on the* $s = 0.63$ *flux surface for one field period (*$0 < \phi < 2\pi/3$*). The local shear value for some contours is marked.*

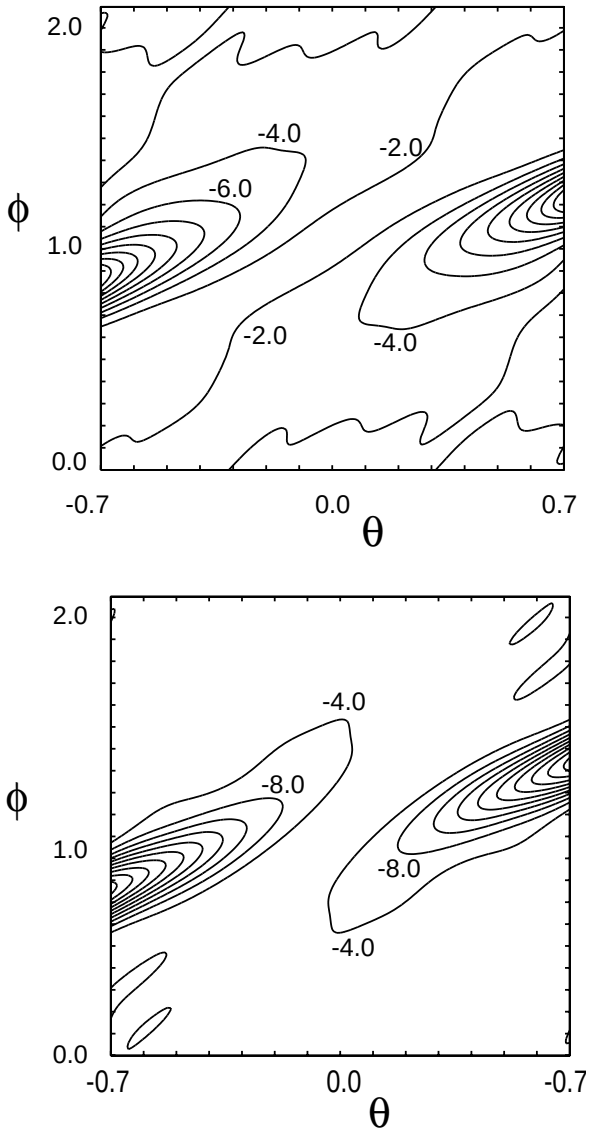

FIG. 9. *The contour plot of the local magnetic shear for the configuration c3m (upper) and c82 (lower) on the* $s = 0.63$ *flux surface on the outboard side of the torus (* $-0.7 < \theta < 0.7$*). The local shear value for some contours is marked.*

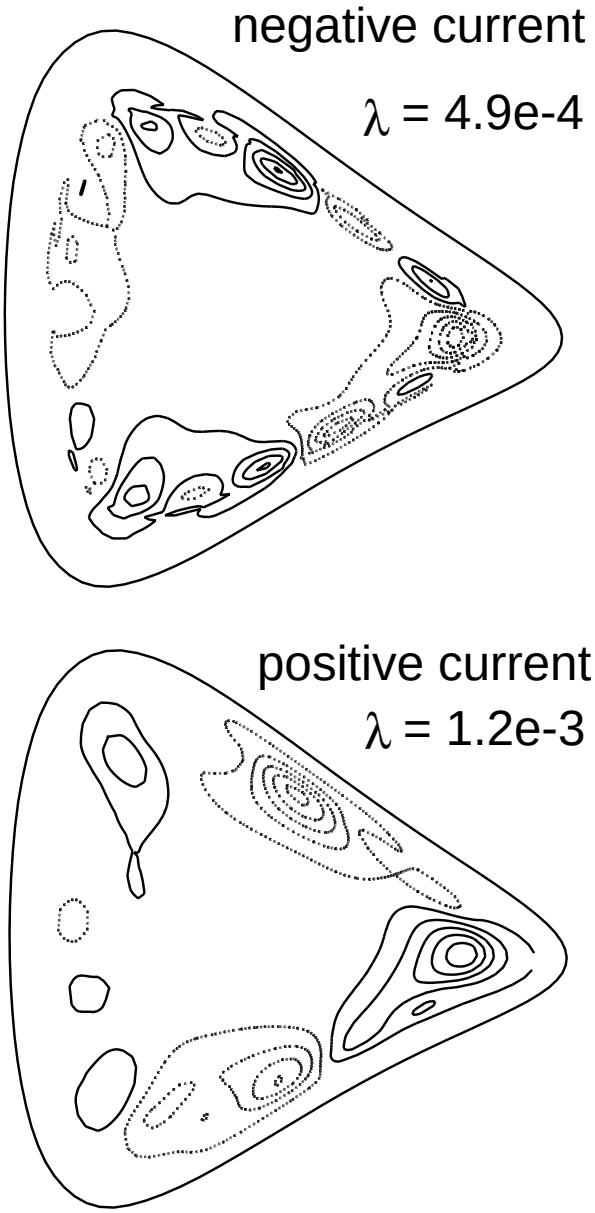

FIG. 10. *The perturbed pressure contours of the $n = 1$ family mode at the $\phi = \pi$ cross-section in a QOS configuration. The upper plot shows a interchange-like internal mode structure. The lower plot shows a kink-ballooning external mode structure obtained when the sign of the bootstrap current is artificially switched.*

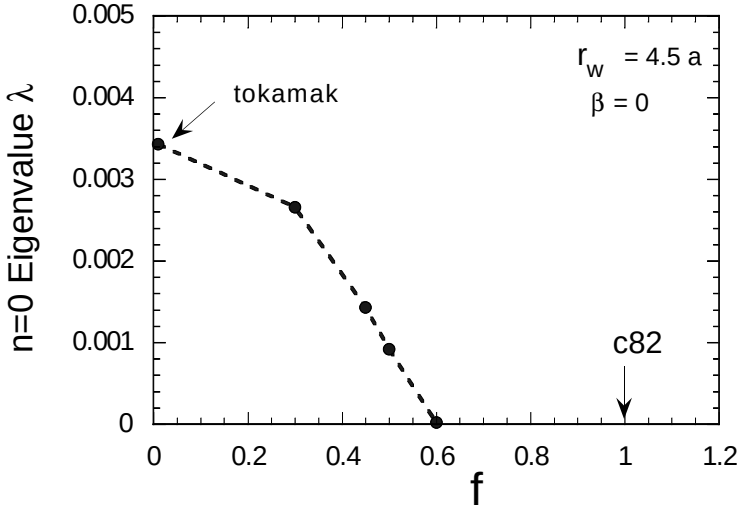

FIG. 11. *The eigenvalue of the vertical mode versus fraction of c82's nonaxisymmetric shape*

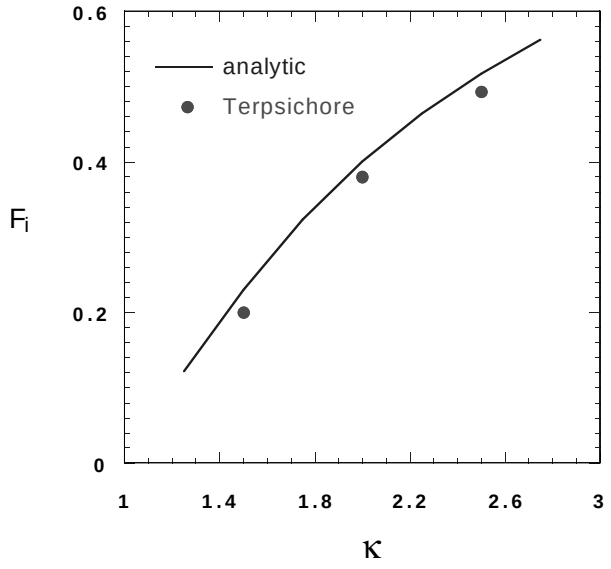

FIG. 12. *The critical value of fraction of external transform as function of axisymmetric elongation*